Characterization of the 2:1 Complex between the Class I MHC-Related Fc Receptor and Its Fc Ligand in Solution†

W. Lance Martin and Pamela J. Bjorkman*

Division of Biology 156-29 and Howard Hughes Medical Institute, California Institute of Technology, Pasadena, California 91125

Received June 11, 1999; Revised Manuscript Received July 26, 1999

ABSTRACT: The neonatal Fc receptor (FcRn) facilitates the transfer of maternal immunoglobulin G (IgG) to offspring and prolongs the half-life of serum IgG. FcRn binds IgG in acidic intracellular vesicles and releases IgG upon exposure to the basic pH of the bloodstream. The crystal structure of an FcRn/Fc complex revealed FcRn dimers bridged by homodimeric Fc molecules to create an oligomeric array with two receptors per Fc [Burmeister et al. (1994) *Nature 372*, 379−383], consistent with the 2:1 FcRn:Fc stoichiometry observed in solution [Huber et al. (1993) *J. Mol. Biol. 230*, 1077−1083; Sánchez et al. (1999) *Biochemistry 38*, 9471−9476]. Two distinct 2:1 FcRn/Fc complexes were present in the cocrystal structure: a complex containing an FcRn dimer interacting with an Fc and a complex in which single FcRn molecules are bound to both sides of the Fc homodimer. To determine which of the two possible 2:1 FcRn/Fc complexes exists in solution, we generated recombinant Fc molecules with zero, one, and two FcRn binding sites and studied their interactions with a soluble form of rat FcRn. The wild-type Fc with two FcRn binding sites binds two FcRn molecules under all assay conditions, and the nonbinding Fc with no FcRn binding sites shows no specific binding. The heterodimeric Fc with one FcRn binding site binds one FcRn molecule, suggesting that the 2:1 FcRn/wild-type Fc complex formed in solution consists of single FcRn molecules binding to both sides of Fc rather than an FcRn dimer binding to a single site on Fc.

The neonatal Fc receptor (FcRn)[1] transports immunoglobulin G (IgG) across epithelial cell barriers. FcRn was originally discovered in the intestine of newborn rodents (reviewed in ref *1*), where it transfers maternal immunoglobulin in ingested milk to the bloodstream of the newborn, thereby allowing passive immunization of the neonate to antigens encountered by the mother. More recently, FcRn has been characterized in adult animals. FcRn in human placenta is thought to transport maternal IgG to the fetus, and recent evidence suggests that FcRn functions throughout life to rescue serum IgG from degradation (reviewed in refs *1*−*3*). In all of its functions, FcRn binds IgG at acidic pH (≤6.5) in intracellular transport vesicles and releases IgG at the basic pH of the blood (pH ∼7.4).

FcRn is a type I membrane glycoprotein consisting of an extracellular domain that resembles class I MHC molecules and a short (43 residue) cytoplasmic tail (*4*). Most biochemical and structural analyses of the FcRn/Fc interaction have been done using a soluble form of the extracellular portion of rat or mouse FcRn, which is composed of the heavy chain extracellular domains (α1, α2, and α3) bound to β2-microglobulin. The crystal structures of soluble FcRn alone (*5*) and of an FcRn/Fc complex (*6*) revealed a dimeric arrangement of receptors. Binding studies involving FcRn mutants with alterations at the dimer interface demonstrated that receptor dimerization is required for high-affinity binding of IgG (*7*, *8*). We therefore suggested that the crystallographically observed dimers represent dimers induced by ligand binding when FcRn is tethered to a membrane (*9*). In the cocrystals, the FcRn dimers are bridged by Fc molecules such that each of the two potential FcRn binding sites on Fc interacts with one of the FcRn molecules in the receptor dimer, resulting in a long "oligomeric ribbon" in which there are two receptors for every Fc dimer (*6*). At micromolar concentrations in solution, there is no detectable formation of the oligomeric ribbon (*10*). Instead, purified FcRn/Fc complexes consist of three molecules: two receptors and one Fc, which presumably represent a portion of the 2*n*:*n* ribbon found in the crystals (*10*, *11*). There are two distinct 2:1 complexes in the cocrystal structure that could account for the FcRn/Fc complex that forms in solution (Figure 1). In one, Fc binds to an FcRn dimer using one of its two potential FcRn binding sites (left shaded portion), and in the other, single FcRn molecules bind to both sides of Fc (right shaded portion). Computational studies suggested that Fc bound to FcRn is bent so as to more optimally contact the FcRn dimer (*12*). A bent, rather than symmetrical, structure of Fc bound to FcRn is compatible with the low-resolution cocrystal structure since the hinge-proximal portions of the C_H2 domain were disordered (*6*). If Fc is distorted when bound

† Supported by a Camille and Henry Dreyfuss Teacher Scholar Award (P.J.B.), a grant from the NIH (AI/GM41239 to P.J.B.), and an NIH predoctoral training grant (5 T32 GM07616 to W.L.M.).

* Corresponding author. Phone: 626 395-8350. Fax: 626 792-3683. E-mail: bjorkman@cco.caltech.edu.

[1] Abbreviations: CHO, Chinese hamster ovary; Fc, Fc fragment from immunoglobulin G; FcRn, Fc receptor, neonatal; hdFc, heterodimer Fc; IgG, immunoglobulin G; K_D, equilibrium dissociation constant; nbFc, nonbinding Fc; RU, resonance units; wtFc, wild-type Fc.

10.1021/bi9913505 CCC: $18.00
Published on Web 09/03/1999

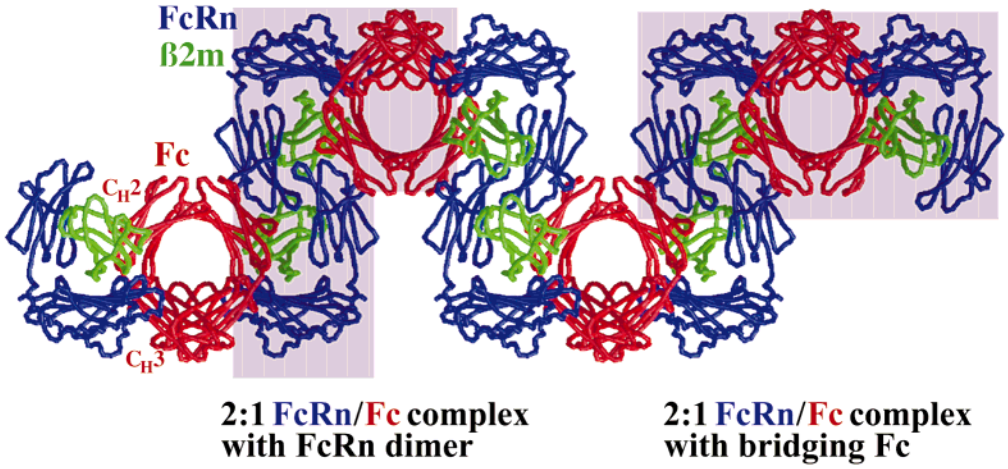

FIGURE 1: FcRn/Fc complexes in the 2n:n oligomeric ribbon observed in the FcRn/Fc cocrystals. FcRn dimers are bridged by homodimeric Fc's. The shaded portions represent the two different 2:1 FcRn/Fc complexes that can be extracted from the ribbon (see text). Although the Fc is depicted as being 2-fold symmetric, the low-resolution FcRn/Fc cocrystal structure did not give information about the location of the hinge-proximal portions of the C_H2 domains since these were disordered (*6*). Computational studies suggest that Fc bends in response to contacting an FcRn dimer (*12*); thus either of the depicted 2:1 FcRn/Fc complexes is a possibility for the 2:1 complex that forms in solution. If the oligomeric ribbon network forms under physiological conditions, each FcRn dimer would be associated with a membrane parallel to the plane of the paper: the left-most dimer is associated with a membrane below the plane of the paper, the central dimer is associated with a membrane above the paper, and the right-most dimer is again associated with the membrane below the plane of the paper.

to an FcRn dimer, a second FcRn might be prevented from binding to the other Fc polypeptide chain in solution. Thus either of the 2:1 FcRn/Fc complexes shown in Figure 1 are a possibility for the complex that forms in solution. To distinguish which 2:1 complex forms in solution, we constructed Fc proteins, similar to those previously expressed by Ward and colleagues (*2*, *13*−*18*), that contain zero, one, or two functional FcRn binding sites and studied their binding to soluble FcRn.

MATERIALS AND METHODS

Construction of Fc Expression Vectors. A rat IgG2a cDNA (kind gift of Mark Agila, University of California, Davis) was modified to encode a secreted Fc fragment as follows: the DNA encoding the V_H and C_H1 domains was removed using loop-out mutagenesis (*19*) to generate an in-frame fusion between the secretion signal sequence and the hinge region. The complete construct encodes the signal sequence fused to IgG2a residues 223−447 (EU numbering; *20*), which corresponds to the hinge, C_H2, and C_H3 domains of wild-type Fc (wtFc). The nonbinding Fc (nbFc) construct was generated from the wtFc construct by introducing mutations at the codons for some of the amino acids previously shown to be critical for FcRn binding (*2*, *9*, *13*−*18*, *21*) to make the following substitutions: Thr252 to Gly, Ile253 to Gly, Thr254 to Gly, His310 to Glu, His433 to Glu, and His435 to Glu. PCR was used to add a factor Xa cleavage site and 6×-His tag to the 3′ end of the nbFc construct (added sequence encodes the following residues C-terminal to residue 447: Gly-Ile-Glu-Gly-Arg-Gly-Ser-Ser-His-His-His-His-His-His). The wtFc and nbFc constructs were subcloned after sequencing into the mammalian cell expression pBJ5-GS (*22*), which carries the glutamine synthetase gene as a means of selection and amplification in the presence of the drug methionine sulfoximine (*23*).

Expression of Fc Proteins. Chinese hamster ovary (CHO) cells were cotransfected with the wtFc and nbFc expression vectors, and selection and amplification of stable cell lines using methionine sulfoximine were carried out as described (*22*, *24*). Successfully transfected cells should secrete a mixture of wtFc and nbFc homodimers and heterodimeric Fc (hdFc) composed of one wtFc and one nbFc polypeptide chain. Cell lines secreting wtFc and hdFc were identified by precipitation at pH 6.0 of [^{35}S]methionine/cysteine (ICN Pharmaceuticals, Inc.) metabolically labeled supernatants using soluble FcRn coupled to CNBr-activated Sepharose beads (Gibco-BRL) (*11*). Bound Fc was eluted from the FcRn-coupled beads by raising the pH to 8.0 and loaded onto a 10% SDS−PAGE gel run under reducing conditions. Bands migrating with apparent molecular masses of 30 and 31 kDa were visualized using a PhosphorImager screen (Molecular Dynamics) (data not shown). The lower band was identified as wtFc by comparison with the Fc protein expressed in cells transfected with the wtFc vector alone (see below). The upper band corresponds to nbFc, which migrates more slowly than wtFc due to addition of the factor Xa site and 6×-His tag to its C-terminus. The majority of the labeled protein migrated as the 30 kDa band, indicating that the FcRn-coupled beads precipitated wtFc homodimers and hdFc. After addition of glycerol to 10%, NaCl to 300 mM, and imidazole to 10 mM, labeled supernatants were also precipitated with Ni−NTA superflow agarose beads (Qiagen). Bound proteins were eluted from the Ni−NTA beads by addition of 1 M imidazole and reducing sample buffer and visualized after SDS−PAGE as described above. The 30 and 31 kDa bands were again present, with the 31 kDa band in excess in this instance, indicating that the nickel beads precipitated His-tagged nbFc homodimers and hdFc.

CHO cells were also transfected with the wtFc expression vector alone. After selection and amplification, cells expressing wtFc homodimers were identified using FcRn-coupled beads as described above.

Purification of Fc Proteins. Secreted wtFc homodimers were isolated from supernatants of CHO cells transfected with only the wtFc expression vector using a modification of a previously described functional purification involving

pH-dependent binding to FcRn immobilized on Sepharose beads (*11*). The pH of the harvested growth media was adjusted to 5.8 with 1 M sodium cacodylate, pH 5.5, (~50 mL/500 mL harvest) then passed over a 10 mL FcRn−Sepharose column at 0.5 mL/min. After washing with 200 mL of 50 mM sodium cacodylate, pH 5.5, 150 mM NaCl, wtFc was eluted with 50 mM Tris-Cl, pH 8.0, 150 mM NaCl, then concentrated, and exchanged into 50 mM Tris-Cl, 50 mM bis-Tris-propane-Cl, pH 8.0. wtFc was loaded onto a Uno-Q1 anion-exchange column (Bio-Rad) mounted on a Biocad 700E perfusion chromatography system (Perkin-Elmer) at 5 mL/min. The Uno-Q1 column was equilibrated with the FcRn loading buffer and then subjected to a pH gradient from 7.5 to 6.0. Under these conditions, wtFc (calculated pI = 7.1) (*25*) does not bind to the column, allowing it to be separated from contaminants that bind. wtFc was concentrated, then purified, and exchanged into 20 mM sodium phosphate, pH 6.0, 150 mM NaCl by flowing it over a Superdex 200 HR 10/30 gel filtration column (Pharmacia) at 0.3 mL/min.

hdFc and nbFc were purified from CHO cells secreting a mixture of wtFc, hdFc, and nbFc. Since only the nbFc polypeptide chain carries a 6×-His tag, hdFc and nbFc bind to a nickel column, whereas wtFc flows through. hdFc and nbFc can then be separated from each other using the FcRn affinity column, which binds hdFc but not nbFc. Harvest media were dialyzed twice using 6000−8000 Da Spectra/Por membranes (Spectrum) against 10 volumes of 20 mM Tris-Cl, pH 8.0, 150 mM NaCl, and 0.05% NaN_3 to remove a media component that stripped nickel from the Ni−NTA column. The harvest media were then supplemented with glycerol to 10%, NaCl to 300 mM, and imidazole to 10 mM. The media were passed over a 20 mL Ni−NTA superflow agarose column at 0.5 mL/min and washed with 200 mL of 50 mM Tris-Cl, pH 8.0, 10% glycerol, 300 mM NaCl, 10 mM imidazole, 0.05% NaN_3. Nickel binding proteins (hdFc and nbFc) were eluted from the column with 50 mM Tris-Cl, pH 8.0, 10% glycerol, 300 mM NaCl, 250 mM imidazole, 0.05% NaN_3. The eluent was concentrated and exchanged into 20 mM sodium cacodylate, pH 5.5, 150 mM NaCl and passed over an FcRn−Sepharose column, which was eluted by raising the pH to 8.0. To avoid potential contamination of the hdFc with wtFc, different FcRn−Sepharose columns were used for purifying wtFc and hdFc. After passing the flow-through over the FcRn−Sepharose column again, the flow-through (nbFc) and the eluent (hdFc) were each loaded onto the Uno-Q1 anion-exchange column as described for wtFc. The hdFc (calculated pI = 6.9) (*25*) binds to the column and elutes at pH 7.4, 6 mL after the wtFc peak. The nbFc (calculated pI = 6.7) (*25*) binds to this column and elutes at pH 7.1, 10 mL after the hdFc peak. In addition to enhancing purity of the samples, this chromatography facilitates evaluation of the degree to which each Fc is free of other contaminating Fc species. Following anion exchange, nbFc and hdFc were concentrated and further purified by gel filtration on a Superdex 200 HR 10/30 column as described for wtFc.

Final yields for the purified Fc proteins ranged from 3 to 7 mg/L of harvest.

Expression and Purification of Soluble FcRn. The FcRn used for these studies was the previously described soluble form of the rat FcRn extracellular region (residues 1−269 of the mature FcRn heavy chain bound to rat β2-microglobulin) produced in CHO cells (*22*). FcRn was isolated from harvested growth media using a functional purification involving pH-dependent binding to an IgG affinity column (*22*). The protein was further purified on Uno-Q1 anion-exchange and Superdex 200 HR 10/30 gel filtration columns and exchanged into assay buffer as described for wtFc.

Determination of Protein Concentrations. FcRn and Fc concentrations were determined spectrophotometrically using extinction coefficients at 280 nm of 84 900 M^{-1} cm^{-1} (FcRn) and 60 900 M^{-1} cm^{-1} (wtFc, hdFc, and nbFc). Extinction coefficients that are valid for denatured protein were first calculated from the protein sequences as described (*26*); then A_{280} measurements for a fixed amount of each protein were compared in 6.0 M GuHCl and aqueous solutions, and the coefficient was adjusted if necessary.

Coprecipitation of FcRn and Fc. Fc proteins were analyzed for their ability to bind simultaneously to more than one FcRn using a modification of a previously described column binding assay (*11*). For each reaction, 20 μL of FcRn−Sepharose beads was washed and resuspended in 50 μL of sodium phosphate, pH 6.0, 150 mM NaCl in a 1.7 mL Eppendorf tube and then incubated with 20 μg of wtFc, nbFc, or hdFc in ~5 μL or with 5 μL of buffer. After washing twice, the beads were resuspended in 50 μL of the same buffer including 20 μg of soluble FcRn. After two subsequent washes, the proteins bound to the beads were eluted with 16 μL of 1 M Tris-Cl, pH 8.0. Eluted proteins were run on a 10% SDS−PAGE gel under reducing conditions and stained with Coomassie brilliant blue.

Nonequilibrium Gel Filtration. The stoichiometry of FcRn/Fc complexes was determined using conventional gel filtration chromatography under nonequilibrium conditions as described (*10*). FcRn was incubated with the various Fc's at molar ratios between 3:1 and 1:1 in 20 mM sodium phosphate, pH 6.0, 150 mM NaCl, keeping the concentration of Fc fixed at 10 μM. After 20 min at room temperature, 25 μL was injected onto a Superdex 200 PC 3.2/30 gel filtration column (Pharmacia) equilibrated in the sodium phosphate buffer, which was run at 0.1 mL/min using a SMART micropurification system (Pharmacia). The absorbance of the eluent was monitored at 280 nm, and fractions were analyzed by SDS−PAGE (data not shown).

Equilibrium Gel Filtration. The equilibrium column chromatography method of Hummel and Dreyer (*27*) and a SMART micropurification system were used to analyze the association of FcRn with the Fc proteins at equilibrium as previously described (*10*). A Superdex 200 PC 3.2/30 gel filtration column was equilibrated with and run in 20 mM sodium phosphate, pH 6.0, 150 mM NaCl containing 2 μM FcRn (equilibration buffer) at 0.1 mL/min. Samples (20 μL) including a 2 μM amount of one of the Fc's and various concentrations of FcRn were incubated for 20 min at room temperature in equilibration buffer that contained 2 μM FcRn. Samples were injected onto the column, and the absorbance of the eluent was monitored at 280 nm.

Biosensor Assays. A BIAcore 2000 biosensor system (Pharmacia, LKB Biotechnology) was used to assay the interaction of FcRn with the Fc molecules. This system includes a biosensor chip with a dextran-coated gold surface to which one protein (referred to as the "ligand") is covalently immobilized. Binding of an injected protein (the "analyte")

to the immobilized protein results in changes that are directly proportional to the amount of bound protein and read out in real time as resonance units (RU) (*28, 29*). FcRn or one of the Fc's was covalently immobilized to three of the four flow cells on a CM5 biosensor chip (Pharmacia) using standard primary amine coupling chemistry (BIAcore manual). Each protein was coupled at three different densities (~200, ~400, and ~1500 RU), and the fourth flow cell was mock coupled using buffer to serve as a blank. For deriving kinetic constants, we used binding experiments conducted for short times (30 s) using fast flow rates (100 μL/min) over flow cells coupled at low density (~200 or ~400 RU). These conditions were chosen to minimize mass transport effects upon the kinetics of binding reactions (*30*). Kinetic constants were derived from the sensorgram data using BIAevaluation version 3.0, which simultaneously fits the association and dissociation phases of the sensorgrams and globally fits all curves in the working set. Sensorgrams were fit to models supplied by the BIAevaluation 3.0 package: the "Langmuir binding" model (a single class of noninteracting binding sites in a 1:1 binding interaction), the "heterogenenous ligand" model (two or more populations of noninteracting binding sites), and the "bivalent analyte" model (the injected protein can bind to two immobilized proteins) (see Figure 5 legend). The appropriate model was chosen on the basis of the quality of the fit to the data, the robustness of the fit under different experimental conditions, and consistency between the binding model and structural information regarding the binding mechanism. Equilibrium dissociation constants (K_D's) were derived from the ratios of rate constants ($K_D = k_d/k_a$, where k_a and k_d are the association and dissociation rate constants, respectively). For some of the binding interactions, we also derived K_D's using an equilibrium-based approach that is not affected by mass transport effects. In these experiments, binding reactions were allowed to closely approach or to reach equilibrium. K_D's were derived by nonlinear regression analysis of plots of R_{eq} (the equilibrium binding response) versus the log of the analyte concentration. The fit of data to binding models assuming a bivalent analyte (A. P. West, unpublished results) or to one or more classes of noninteracting binding sites on the ligand was examined, and the appropriate model was chosen as described (*31*). For each analysis, the bulk refractive index parameter was set to zero for every concentration.

RESULTS

wtFc and hdFc, but Not nbFc, Bind to FcRn. In previous studies by Ward and colleagues, recombinant versions of wild-type (two FcRn binding sites), nonbinding (zero FcRn binding sites), and heterodimeric (one FcRn binding site) mouse Fc were produced in bacteria (*13*−*15*). These proteins were used for in vivo catabolic and transcytosis studies, as well as for biochemical analyses of binding to soluble mouse FcRn (*13*−*15, 17, 18, 32, 33*). The heterodimeric Fc was shown to bind mouse FcRn (*33*), but it was not protected from serum degradation or transported across the mouse intestine as efficiently as wild-type Fc (*13, 14*). We expressed analogous versions of rat Fc in stably transfected CHO cells in order to generate milligram quantities of glycosylated Fc fragments that could be used for crystallographic and biochemical studies involving soluble FcRn.

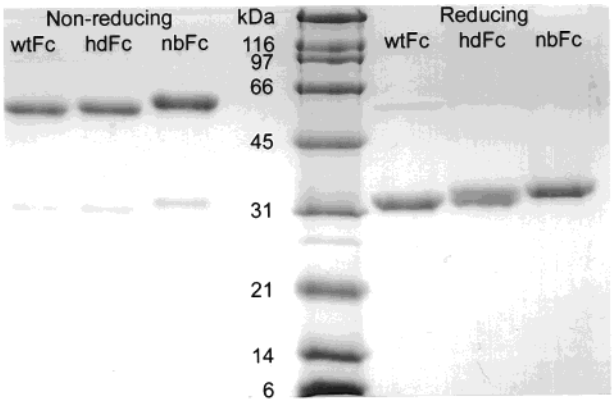

FIGURE 2: SDS−PAGE analysis of Fc proteins. Samples were run under reducing or nonreducing conditions on a 10% SDS−PAGE gel.

CHO cells were cotransfected with expression vectors encoding a secretion signal sequence followed by the hinge, C_H2, and C_H3 domains of wtFc and nbFc derived from a rat IgG2a gene. The nbFc construct was generated from the wtFc construct by introduction of a C-terminal 6×-His tag sequence and incorporation of substitutions identified previously that reduce or eliminate binding of Fc to FcRn (*2, 9, 13*−*18, 21*). FcRn- and nickel-based precipitation methods were used to identify transfected cells that secrete a mixture of wtFc homodimers, nbFc homodimers, and hdFc molecules (data not shown).

The purification procedures used to isolate the Fc's require that wtFc and hdFc bind to FcRn at pH 6 but not pH 8, as observed for IgG (*34*), and that nbFc be unable to bind to FcRn. hdFc and nbFc were purified from the harvested growth media of stably cotransfected cells using a combination of nickel and FcRn−Sepharose chromatography. Supernatants were first passed over a Ni−NTA column, which binds nbFc and hdFc. The eluted proteins were then run over an FcRn−Sepharose column at pH 6 to separate nbFc and hdFc. nbFc was further purified from the flow-through of this column, whereas hdFc was purified after elution at pH 8 from the FcRn−Sepharose column. To obtain large quantities of wtFc, this protein was purified from the harvested growth media of cells transfected with the wtFc expression vector only, using pH-dependent binding to the FcRn−Sepharose column. SDS−PAGE analysis of the purified Fc's under reducing conditions revealed single bands at the expected molecular weights for nbFc and wtFc and two bands corresponding to the nbFc and wtFc polypeptide chains for the hdFc (Figure 2). Under nonreducing conditions, each protein migrates as a dimer, demonstrating that the hinge region interchain disulfide bonds had formed correctly (Figure 2). N-Terminal sequence analysis of purified hdFc revealed a single amino acid sequence (Val-Pro-Arg-Glu-X-Asn-Pro-X-Gly-X, where X corresponds to cysteine, which was not determined using this protocol) (data not shown). This sequence corresponds to residues 223−232 of Fc, demonstrating that the secretion signal sequence had been properly cleaved from the wtFc and nbFc polypeptide chains.

wtFc and hdFc Show Different Properties When Binding to Immobilized FcRn. We previously used a column binding assay to show that more than one FcRn molecule can bind to purified rat Fc (*11*). In this experiment, soluble rat FcRn

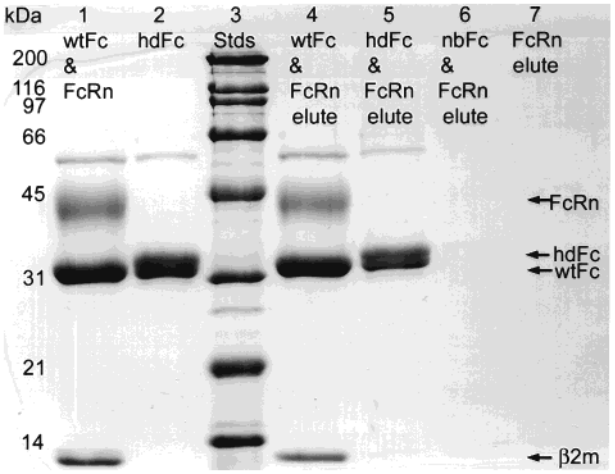

FIGURE 3: SDS−PAGE analysis of proteins eluted from immobilized FcRn. Samples were run under reducing conditions on a 10% SDS−PAGE gel. Lanes 1 and 2: 5 μg of each of the indicated proteins. Lanes 4−7: Proteins eluted from FcRn−Sepharose when incubated with the following proteins (20 μg each): wtFc and FcRn (lane 4), hdFc and FcRn (lane 5), nbFc and FcRn (lane 6), and FcRn (lane 7). Only wtFc is able to bind simultaneously to immobilized FcRn and added soluble FcRn (lane 4). hdFc bound to immobilized FcRn does not bind additional FcRn molecules (lane 5). nbFc and FcRn (lane 6) or FcRn alone (lane 7) does not bind to immobilized FcRn.

was covalently coupled to Sepharose beads and used to bind Fc at pH 6.0. When additional FcRn was passed over the column, it bound to the FcRn/Fc complex, indicating that more than one FcRn molecule could bind to a single Fc (*11*). In the present study, we performed a precipitation-based version of this experiment using wtFc and hdFc. As demonstrated previously (*11*), wtFc is capable of binding simultaneously to immobilized FcRn on the beads and to soluble FcRn, but no detectable soluble FcRn binds to immobilized FcRn in the absence of added Fc (Figure 3). By contrast, hdFc binds to immobilized FcRn but does not bind additional soluble FcRn, suggesting that hdFc can only bind to a single FcRn under the conditions of this experiment. As expected, no detectable nbFc bound to the immobilized FcRn (Figure 3).

Gel Filtration Analyses Demonstrate Different Stoichiometries for wtFc and hdFc Binding to FcRn. We previously described nonequilibrium and equilibrium gel filtration assays to determine the stoichiometry of rat and mouse FcRn complexes with Fc (*10*). In the present study, we compared the properties of wtFc, hdFc, and nbFc in these assays. In the nonequilibrium-based experiments, various ratios of FcRn and one of the Fc's were incubated at pH 6.0, and the FcRn/Fc complex was separated from the free proteins on a gel filtration column. There was no detectable complex formed when mixtures of nbFc and FcRn were chromatographed together on the column (data not shown). For wtFc, we obtained results similar to those previously reported (*10*), such that virtually all of the protein chromatographs as the complex at a 2:1 molar ratio of FcRn to Fc (Figure 4A). When the input ratio of FcRn to wtFc is greater than 2:1, there is an additional peak corresponding to free FcRn; when the input ratio of FcRn to wtFc is less than 2:1, there is an additional peak corresponding to free wtFc (verified by SDS−PAGE; data not shown). By contrast, for hdFc, the

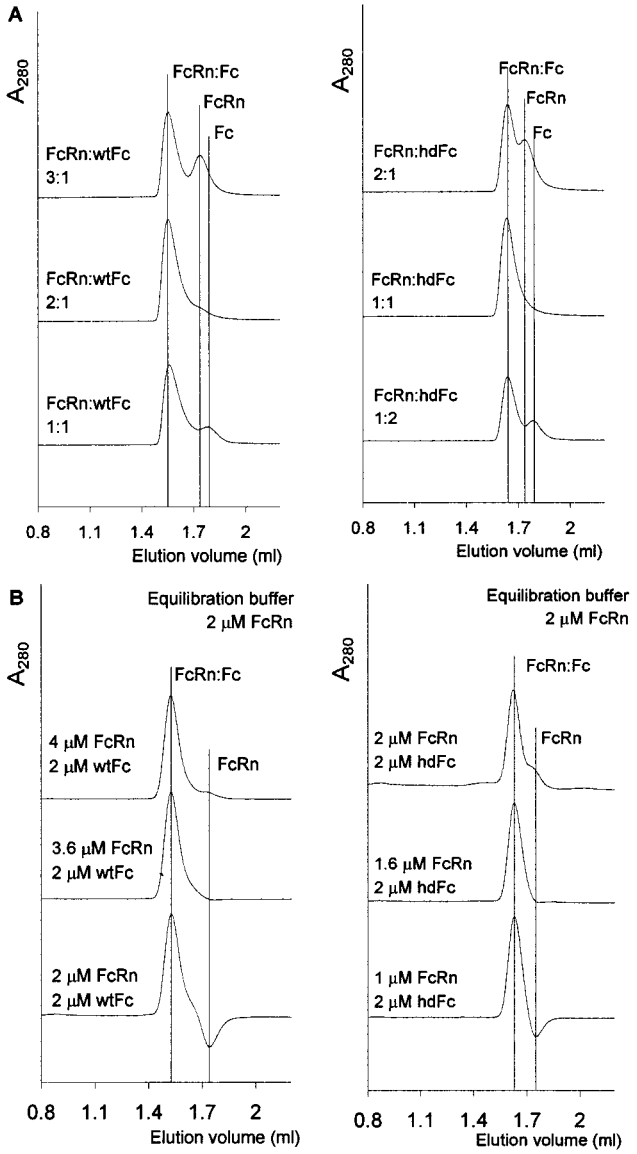

FIGURE 4: Gel filtration analyses of FcRn/Fc complexes. (A) Nonequilibrium gel filtration. FcRn and wtFc or hdFc were incubated at pH 6.0 at the indicated molar ratios and then passed over a gel filtration column run under nonequilibrium conditions to separate FcRn/Fc complexes from the free proteins. The identities of the proteins in each peak were confirmed by SDS−PAGE (data not shown). A single peak corresponding to an FcRn/Fc complex is formed at a 2:1 stoichiometry for FcRn/wtFc and a 1:1 stoichiometry for FcRn/hdFc. (B) Equilibrium gel filtration. FcRn was incubated with 2 μM wtFc or 2 μM hdFc at the indicated FcRn/Fc ratios in buffer containing 2 μM FcRn (equilibration buffer). Samples were injected onto a column equilibrated in the equilibration buffer. The peak that elutes first corresponds to an FcRn/Fc complex in equilibrium with free Fc; thus the concentration of bound Fc in the complex is lower than 2 μM. The second peak or trough is at the elution volume of free FcRn. Under equilibrium conditions, the stoichiometry of the solution complex can be determined from the chromatogram with a flat baseline by rounding up the ratio of injected proteins to the nearest integral value. Thus FcRn binds to wtFc with 2:1 stoichiometry and to hdFc with 1:1 stoichiometry under these conditions.

proteins chromatograph as a complex at a 1:1 molar ratio (Figure 4A).

Stoichiometries determined using conventional gel filtration are not definitive because the protein−protein complex is being assayed under nonequilibrium conditions. Thus if some of the complexes dissociate during the experiment, their

constituents can fail to rebind because they are being separated from each other during the chromatographic procedure. For example, high mannose carbohydrate-containing forms of mouse FcRn can form 1:1 complexes with Fc when assayed under nonequilibrium conditions (*10*, *33*) but form 2:1 complexes when evaluated under equilibrium conditions (*10*). We therefore used the equilibrium gel filtration method of Hummel and Dreyer (*27*) to investigate the interactions of wtFc and hdFc with FcRn. As previously described (*10*), we equilibrated a gel filtration column with buffer containing a uniform concentration of FcRn. Pre-equilibrated complexes of FcRn plus Fc in different ratios were then injected over the gel filtration column. If the amount of additional FcRn injected with Fc is greater than or less than the amount required for formation of the FcRn/Fc complex, there is a peak (in the case of too much FcRn) or a trough (in the case of too little FcRn) at the position where free FcRn migrates. When the amount of additional FcRn injected with Fc is equal to the amount required for forming the FcRn/Fc complex, there is a flat baseline at the position where free FcRn migrates. Unless the protein concentrations greatly exceed the K_D of the interaction, however, the ratio of the concentration of added FcRn to the concentration of Fc will be a nonintegral value, from which the integral value corresponding to the stoichiometry generally can be derived by rounding up to the next integer. This is because the peak corresponding to the complex contains significant amounts of free Fc in equilbrium with the bound form, unless the experiment is conducted at concentrations that exceed the K_D by greater than 10-fold, which is usually not possible due to limiting amounts of purified protein.

We equilibrated a small (2.4 mL total volume) gel filtration column with 2 μM FcRn. Samples containing 2 μM wtFc or hdFc were incubated with various amounts of FcRn and chromatographed in the equilibration buffer containing FcRn. As shown in Figure 4B, a flat baseline is observed at the position where free FcRn migrates when 3.6 μM additional FcRn is injected with 2 μM wtFc; thus the stoichiometry of the FcRn/wtFc interaction is 2:1 under equilibrium conditions. By contrast, a flat baseline is observed when 1.6 μM hdFc is injected with 2 μM hdFc; thus at concentrations up to 2 μM, hdFc interacts with only one FcRn molecule (Figure 4B). The nbFc shows no specific interaction with FcRn (data not shown).

Comparison of wtFc and hdFc Binding to FcRn Using Surface Plasmon Resonance Assays. FcRn was covalently immobilized onto the surface of a biosensor chip, and binding of the Fc proteins was monitored in real time using a surface plasmon resonance-based binding assay, as previously described (*7*, *8*, *21*, *31*, *35*). We first analyzed the ability of nbFc to bind FcRn to check for residual binding at high concentrations. We found that nbFc does not generate a net binding response unless it is injected at concentrations exceeding 5 μM. At these concentrations, the responses are independent of concentration and are not reproducible from flow cell to flow cell or from chip to chip and thus represent nonspecific interactions with the biosensor chip (data not shown). For wtFc, the binding data were fit to a simple 1:1 interaction model and to a more complex model that assumes the response is due to two independent classes of noninteracting binding sites (heterogeneous ligand model) (Figure 5A). The heterogeneous ligand model fit the data better, as found in previous biosensor-based studies using intact IgG or Fc fragments (*31*). Using the heterogeneous ligand model, we derive a K_D of 1−6 nM for the high-affinity population, representing 55% of the binding sites, and a K_D of 143−218 nM for the low-affinity population, representing 45% of the binding sites. By contrast, the hdFc binding data fit the simple 1:1 interaction model quite well with a derived K_D of 75−96 nM (Figure 5A).

Because the hdFc/FcRn binding data fit the simple 1:1 interaction model, we inferred that the complex binding data observed in the wtFc/FcRn interaction result primarily from the presence of two potential FcRn binding sites on wtFc rather than from two populations of FcRn molecules on the chip surface. We therefore modeled the interaction of FcRn and wtFc as one side of wtFc binding the coupled FcRn followed by the wtFc/FcRn complex binding another FcRn using the second FcRn binding site on wtFc (bivalent analyte model). Using this model, a K_D is derived for each binding event, neither of which represents the affinity of wtFc being bound on both sides by FcRn; i.e., both K_D's represent distinct microscopic binding events. When the wtFc binding data are analyzed using this model, the K_D for the first binding event is in the range of 68−116 nM, and the second K_D is 317−487 nM (Figure 5A). Thus the K_D for the binding of FcRn to one site on wtFc is comparable to the 75−96 nM K_D derived for the binding of FcRn to hdFc. From these results, we conclude that the complex response exhibited by the interaction of FcRn with Fc or IgG on a biosensor chip is primarily the result of FcRn binding IgG or Fc at both FcRn binding sites.

We previously noted that the affinities of FcRn/IgG complexes are higher when FcRn, rather than IgG, is immobilized on the biosensor chip (*31*). All IgG subtypes tested showed a systematic coupling-dependent affinity difference, such that the high-affinity K_D when FcRn was immobilized (determined using a two-site heterogeneous ligand model) ranged between 15 and 93 nM, whereas the high-affinity K_D when IgG was immobilized ranged between 74 and 740 nM (*30*). To determine if hdFc exhibited a similar coupling-dependent affinity difference, we compared the binding of FcRn to wtFc and hdFc when each was immobilized to a biosensor chip. In both cases, the binding data could be fit to the simple 1:1 interaction model, and the derived K_D was 450−500 nM (Figure 5B). Thus both hdFc and wtFc bind to FcRn with lower affinity when they are immobilized than when they are injected over immobilized FcRn.

DISCUSSION

FcRn functions in the transport of IgG across epithelia and in the protection of IgG from catabolism in the serum (reviewed in refs *1*−*3*). Crystals of a complex between rat FcRn and the Fc fragment of IgG reveal an extended oligomeric ribbon of FcRn dimers bridged by homodimeric Fc's (*6*) (Figure 1). We have suggested that this ribbon forms under physiological conditions, such as the inside of an acidic transport vesicle, and that ribbon formation could serve as a component of a trafficking signal for directing vesicles containing bound IgG to their correct destination (*9*). To investigate this hypothesis, we have initiated a systematic

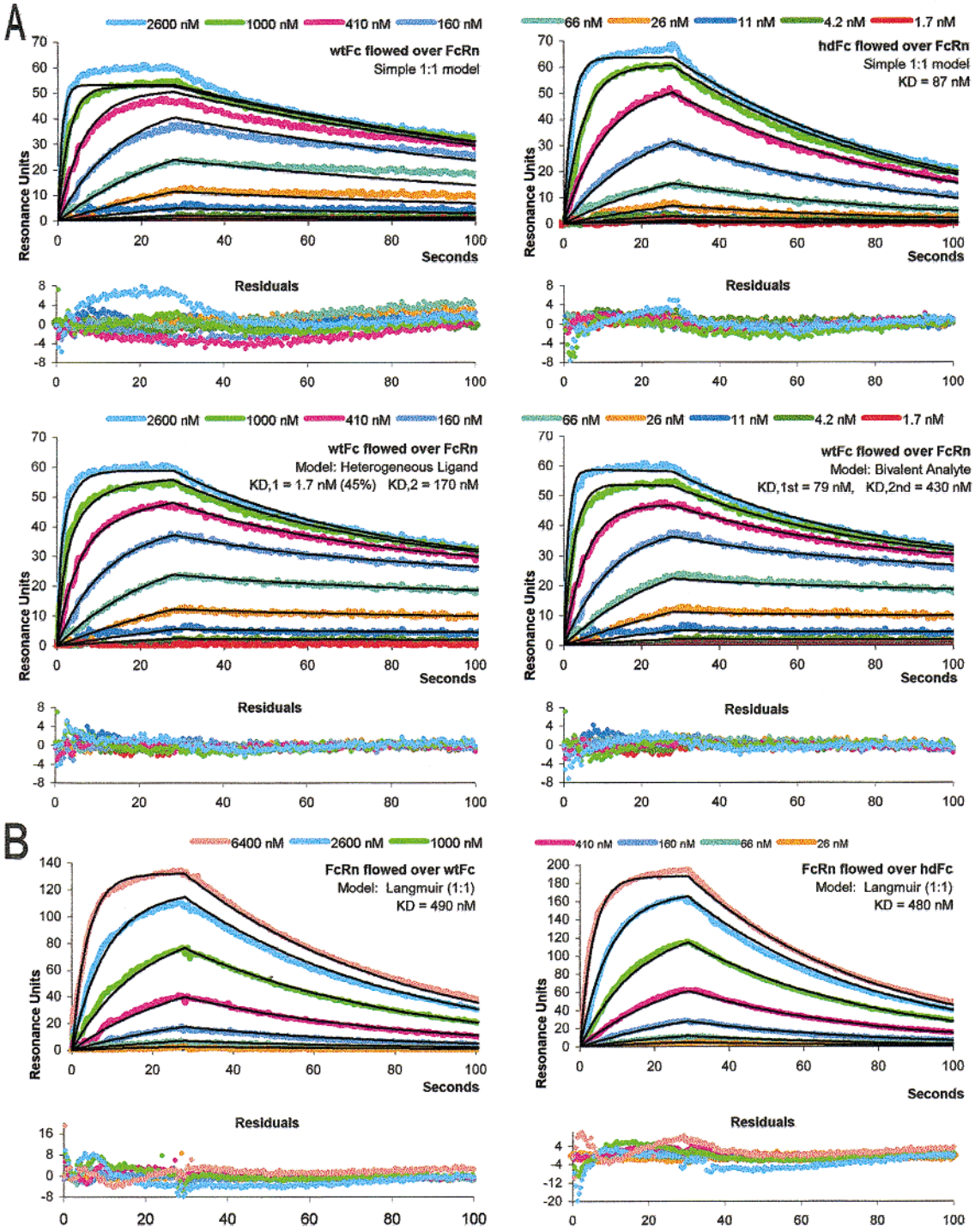

FIGURE 5: Biosensor analyses of FcRn/Fc complexes. FcRn or Fc was coupled to a biosensor chip at ~200, ~400, and ~1500 RU. Sensorgrams (colored lines) were analyzed using a kinetics-based method for the two lower coupling densities. An equilibrium-based method was used for analyses of data from all three coupling densities, yielding results comparable to those of the kinetics-based analyses (data not shown). In each panel, the model used to fit the data (thin black lines overlaid with the observed response) is listed along with derived affinity constant(s). The simple 1:1 model fits the data to the reaction FcRn + Fc ⇔ FcRn:Fc. The heterogeneous ligand model assumes that there are two populations of FcRn on the chip and fits the data according to the following reactions: FcRn + Fc ⇔ FcRn:Fc and FcRn* + Fc ⇔ FcRn*:Fc. K_D's ($K_{D,1}$ or $K_{D,2}$) and the percentage of the total response due to each population of FcRn are derived for each reaction. The bivalent analyte model fits the data according to the following sequential reactions: FcRn + Fc ⇔ FcRn:Fc and FcRn:Fc + FcRn ⇔ FcRn:Fc:FcRn. K_D's ($K_{D,first}$ and $K_{D,second}$) are derived for each reaction. (A) Sensorgrams from kinetics-based experiments in which the indicated Fc is flowed over FcRn. One representative set of injections from experiments performed in duplicate or triplicate is shown for each interaction on a chip coupled to ~400 RU. Similar results were obtained for the ~200 RU coupling density chips (wtFc: $K_{D,1}$ = 4 nM (58%); $K_{D,2}$ = 185 nM (42%); $K_{D,first}$ = 101 nM; $K_{D,second}$ = 336 nM. hdFc: K_D = 86 nM). (B) Sensorgrams from kinetics-based experiments in which FcRn is flowed over the indicated Fc. One representative set of injections from experiments performed in duplicate or triplicate is shown for each interaction on a chip coupled to ~200 RU. Similar results were obtained for the ~400 RU coupling density chips (wtFc: K_D = 500 nM. hdFc: K_D = 460 nM).

characterization of the interaction between FcRn and its Fc ligand.

Many biochemical studies of FcRn, a membrane-bound receptor that normally interacts with its ligand in the lumen of intracellular transport vesicles, have been done in solution using a soluble version of the receptor. Under equilibrium conditions in solution, the FcRn/ligand complex is composed of three molecules, two FcRn's and one Fc (*10*, *11*). In the FcRn/Fc cocrystals, there are two distinct possibilities that could account for the 2:1 complex observed in solution. In one, a dimer of FcRn molecules binds to only one FcRn binding site on homodimeric Fc. In the other, single FcRn molecules bind to both FcRn binding sites on Fc (*6*).

Here we describe the use of recombinant Fc proteins containing zero, one, or two binding sites for FcRn (nbFc, hdFc, and wtFc, respectively) to determine the nature of the FcRn/Fc complex formed in solution. The experimental results consistently demonstrate that the 2:1 FcRn/Fc solution complex consists of two FcRn molecules binding to both sides of wtFc. First, using an assay involving FcRn bound to a solid support, we show that more than one FcRn molecule can bind to wtFc but not to hdFc (Figure 3). In addition, gel filtration analyses under both equilibrium and nonequilibrium conditions demonstrate that hdFc forms a 1:1 complex with FcRn, whereas wtFc forms a 2:1 FcRn/Fc complex (Figure 4). The 1:1 nature of the FcRn complex with hdFc is reflected in biosensor analyses of this interaction, in that binding data involving hdFc could be fit to a simple 1:1 binding model. By contrast, binding data for the interaction of coupled FcRn with wtFc or intact IgG must be fit to more complex binding models that incorporate binding to the second FcRn binding site on Fc (Figure 5A). Combined with a previous demonstration that soluble FcRn is monomeric at micromolar concentrations in solution (*22*), the present results establish that FcRn does not dimerize in solution, either alone or when bound to Fc.

The result that the 2:1 FcRn/Fc complex formed in solution does not include FcRn dimers cannot be used to infer that receptor dimerization does not occur under physiological conditions. In biochemical experiments such as those described here, soluble FcRn is studied at relatively low protein concentrations (micromolar) that would not be expected to favor formation of receptor dimers or the oligomeric ribbon. In vivo, however, receptors are tethered to a membrane under conditions of high effective molarity in which receptor dimerization and oligomeric ribbon formation could be facilitated. Tethering of soluble FcRn to a biosensor chip may to some extent mimic the high local protein concentrations found in a membrane by facilitating dimerization of FcRn. Previous studies suggest that FcRn can dimerize on a biosensor chip, in that mutations at the FcRn dimer interface that do not directly contact IgG resulted in reduced affinities for IgG (*8*). In addition, the previous observation that the affinity between FcRn and Fc or IgG is highest when the receptor rather than the ligand is coupled to a biosensor chip (*31*) can now be interpreted by assuming that FcRn can dimerize when coupled to a biosensor chip. This orientation effect is not due to the ability of FcRn to bind IgG and wtFc at two sites because it is also produced by hdFc, which can only be bound on one side by FcRn. A reasonable explanation for this effect is that FcRn can form dimers when coupled to the surface of the biosensor chip at high effective molarity and that these dimers bind Fc and IgG more stably than does monomeric FcRn, which is the predominant species binding to immobilized Fc or IgG.

The use of Fc molecules that contain zero, one, or two FcRn binding sites has allowed the identification of the trimolecular 2:1 FcRn/Fc complex that forms under micromolar conditions in solution. Future studies of the interaction of these Fc molecules with membrane-bound FcRn will facilitate understanding of the more complex interactions between this receptor and its ligand under physiological conditions.

ACKNOWLEDGMENT

We thank Gary Hathaway and the Caltech PPMAL for microchemical analyses, Anthony West and Luis Sánchez for helpful discussions, and members of the Bjorkman laboratory for critical reading of the manuscript.

REFERENCES

1. Junghans, R. P. (1997) *Immunol. Res. 16*, 29−57.
2. Ghetie, V., and Ward, E. S. (1997) *Immunol. Today 18*, 592−598.
3. Simister, N. E., Israel, E. J., Ahouse, J. C., and Story, C. M. (1997) *Biochem. Soc. Trans. 25*, 481−486.
4. Simister, N. E., and Mostov, K. E. (1989) *Nature 337*, 184−187.
5. Burmeister, W. P., Gastinel, L. N., Simister, N. E., Blum, M. L., and Bjorkman, P. J. (1994) *Nature 372*, 336−343.
6. Burmeister, W. P., Huber, A. H., and Bjorkman, P. J. (1994) *Nature 372*, 379−383.
7. Raghavan, M., Chen, M. Y., Gastinel, L. N., and Bjorkman, P. J. (1994) *Immunity 1*, 303−315.
8. Vaughn, D. E., Milburn, C. M., Penny, D. M., Martin, W. L., Johnson, J. L., and Bjorkman, P. J. (1997) *J. Mol. Biol. 274*, 597−607.
9. Raghavan, M., and Bjorkman, P. J. (1996) *Annu. Rev. Cell Biol. 12*, 181−220.
10. Sánchez, L. M., Penny, D. M., and Bjorkman, P. J. (1999) *Biochemistry 38*, 9471−9476.
11. Huber, A. H., Kelley, R. F., Gastinel, L. N., and Bjorkman, P. J. (1993) *J. Mol. Biol. 230*, 1077−1083.
12. Weng, Z., Gulukota, K., Vaughn, D. E., Bjorkman, P. J., and DeLisi, C. (1997) *J. Mol. Biol. 282*, 217−225.
13. Kim, J.-K., Tsen, M.-F., Ghetie, V., and Ward, E. S. (1994) *Eur. J. Immunol. 24*, 2429−2434.
14. Kim, J.-K., Tsen, M.-F., Ghetie, V., and Ward, E. S. (1994) *Scand. J. Immunol. 40*, 457−465.
15. Kim, J. K., Tsen, M. F., Ghetie, V., and Ward, E. S. (1994) *Eur. J. Immunol. 24*, 542−548.
16. Ghetie, V., Popov, S., Borvak, J., Radu, C., Matesoi, D., Medesan, C., Ober, R. J., and Ward, E. S. (1997) *Nat. Biotechnol. 15*, 637−640.
17. Medesan, C., Matesoi, D., Radu, C., Ghetie, V., and Ward, E. S. (1997) *J. Immunol. 158*, 2211−2217.
18. Medesan, C., Cianga, P., Mummert, M., Stanescu, D., Ghetie, V., and Ward, E. S. (1998) *Eur. J. Immunol. 28*, 2092−2100.
19. Kunkel, T. A., Roberts, J. D., and Zakour, R. A. (1987) *Methods Enzymol. 154*, 367−382.
20. Kabat, E. A., Wu, T. T., Perry, H. M., Gottesman, K. S., and Foeller, C. (1991) *Sequences of proteins of immunological interest*, U.S. Department of Health and Human Services, Bethesda, MD.
21. Raghavan, M., Bonagura, V. R., Morrison, S. L., and Bjorkman, P. J. (1995) *Biochemistry 34*, 14649−14657.
22. Gastinel, L. N., Simister, N. E., and Bjorkman, P. J. (1992) *Proc. Natl. Acad. Sci. U.S.A. 89*, 638−642.
23. Bebbington, C. R., and Hentschel, C. C. G. (1987) The use of vectors based on gene amplification for the expression of cloned genes in mammalian cells, in *DNA Cloning: A*

Practical Approach (Glover, D. M., Ed.) pp 163−188, IRL Press, Oxford.
24. Chapman, T. L., and Bjorkman, P. J. (1997) *J. Virol.* (in press).
25. GCG, W. (1994) *Program manual for the Wisconsin Package*, Genetics Computer Group, Madison, WI.
26. Gill, S. C., and Von Hippel, P. H. (1989) *Anal. Biochem. 182*, 319−326.
27. Hummel, J. P., and Dreyer, W. J. (1962) *Biochim. Biophys. Acta 63*, 530−532.
28. Fägerstam, L. G., Frostell-Karlsson, A., Karlsson, R., Persson, B., and Rönnber, I. (1992) *J. Chromatogr. 597*, 397−410.
29. Malmqvist, M. (1993) *Nature 361*, 186−187.
30. Karlsson, R., and Fält, A. (1997) *J. Immunol. Methods 200*, 121−133.
31. Vaughn, D. E., and Bjorkman, P. J. (1997) *Biochemistry 36*, 9374−9380.
32. Ghetie, V., Hubbard, J. G., Kim, J.-K., Tsen, M.-F., Lee, Y., and Ward, E. S. (1996) *Eur. J. Immunol. 26*, 690−696.
33. Popov, S., Hubbard, J. G., Kim, J.-K., Ober, B., Ghetie, V., and Ward, E. S. (1996) *Mol. Immunol. 33*, 521−530.
34. Rodewald, R., and Kraehenbuhl, J.-P. (1984) *J. Cell Biol. 99*, S159−S164.
35. Raghavan, M., and Bjorkman, P. J. (1995) *Structure 3*, 331−333.

BI9913505